Cement and Concrete Research 42 (2012) 327–332

Contents lists available at SciVerse ScienceDirect

Cement and Concrete Research

journal homepage: http://ees.elsevier.com/CEMCON/default.asp

# Change in reaction kinetics of a Portland cement caused by a superplasticizer — Calculation of heat flow curves from XRD data

D. Jansen [a,*], J. Neubauer [a,*], F. Goetz-Neunhoeffer [a], R. Haerzschel [b], W.-D. Hergeth [b]

[a] Mineralogy, GeoZentrum Nordbayern, University of Erlangen-Nuremberg, D-91054 Erlangen, Germany
[b] Wacker Chemie AG, Muenchen, Germany

ARTICLE INFO

*Article history:*
Received 22 June 2011
Accepted 11 October 2011

*Keywords:*
OPC
Hydration
Superplasticizer
X-ray diffraction

ABSTRACT

The hydration process of a commercial Portland cement was followed by means of heat flow calorimetry. The measured heat flow was compared with calculated heat flow curves based on XRD data. Examined in particular was the influence of one selected superplasticizer on the hydration of the Portland cement. It was shown that the superplasticizer in question retards both the aluminate reaction and the silicate reaction. It is certainly conceivable that there are more than only one explanation for the interaction between the superplasticizer and the cement. A complexation of $Ca^{2+}$ ions from pore solution by the superplasticizer is as thinkable as the adsorption of the polymer on the nuclei or the anhydrous grain surfaces which in turn might lead to the prevention of the growth of the nuclei or the dissolution of the anhydrous grains.



## 1. Introduction

Superplasticizers (SP) are an irreplaceable compound for construction chemistry inasmuch as they improve the workability and flowability of concrete and mortar. They can be used in order to produce modern products such as self levelling compounds [1] and high performance concrete [2]. When they are used in concrete a reduction of the water content can result in improved mechanical properties [3]. If superplasticizers are added to binders without reducing the water content an improved flowability is achieved. This improved flowability is a fundamental requirement for self leveling underlayments or screeds.

Modern superplasticizers in cementitious systems are comb-shaped polycarboxylate-ethers. The liquefaction of the paste is caused by the adsorption of the large molecules on the surfaces of the inorganic grains (cement particles, aggregate). Repulsive forces obtaining between the different grains hinder coagulation and sedimentation and ensure a liquid-like rheology. The role of the different forces (steric or electrostatic) acting in the cement pastes where superplasticizers are present is also a topic of scientific debate and has already been discussed in detail [6,7].

Much research has been performed concerning the effects of superplasticizers on the hydration of cement in general, and their effects on the morphology and the microstructural development of hardened cementitious products in particular. These findings are summarized in several review articles [4,5,11].

Like many organic compounds, superplasticizers have an impact on the hardening process of the inorganic binder cement. These interactions can lead to undesired effects, such as unintended retardation of the whole product, early slump loss, or poor flow behavior. Hence, many efforts have been undertaken to examine the compatibility or incompatibility of different cements with different superplasticizers [8–10].

In the past, much research on the interaction of superplasticizers with hydrating cements was focused on adsorption and rheology experiments [20–23].

Research has also been focused on the chemical structure of the superplasticizers. Winnefeld et al. [24] have investigated the interaction between polycarboxylate superplasticizers with different molecular structures and hydrating Portland cements. They concluded that the duration of the dormant period during cement hydration with SP added is a function of charge density and of the side chain density of the SPs used. Yamada et al. [25] concluded that longer side chains, combined with shorter mean backbone chains, give more fluidity at the same dosage.

Models for the interaction between superplasticizers and cements range from preferred adsorption and intercalation of parts of said large molecules [14] to interaction of macromolecules with ions in the pore solution of the cement/mortar/concrete-paste.

Yoshioka [12] and Plank [13] showed that the adsorption of the superplasticizers on the surfaces of cement particles depends on the surface charge of said particles. Hence, superplasticizers preferentially adsorb on the surface of minerals displaying opposite charge in solution, such as $C_3A$ and ettringite.

Another focus of research has been the influence of superplasticizers on the reaction rate of cements and cement phases. It has been

* Corresponding authors. Tel.: +49 9131 85 23986; fax.: +49 9131 85 23734.
*E-mail addresses:* DanHerJansen@googlemail.com (D. Jansen), neubauer.gzn@me.com (J. Neubauer).

0008-8846/$ – see front matter © 2011 Elsevier Ltd. All rights reserved.
doi:10.1016/j.cemconres.2011.10.005

shown that polycarboxylate superplasticizers retard the dissolution of the phase alite as a function of charge density [15,16]. However, several authors concur in finding that the superplasticizer exerts no effect on the composition of the pore solution [16].

In contrast to these findings, Plank and Larbi [17–19] assumed an interaction of superplasticizers as well as latexes with cations in a pore solution displaying opposite charge, though a difference in $Ca^{2+}$ concentration in pore solution could not be detected within the first 24 h of hydration when adding a superplasticizer.

The present work focuses, from a mineralogical point of view, on the tracking of the retardation process, caused by a superplasticizer, of a commercial OPC. To this end X-ray diffraction techniques were combined with heat flow experiments. The evolution of the sample hardness was also tracked using a Gillmore needle apparatus (Fig. 1).

## 2. Experimental

A special linear polycarboxylate-based superplasticizer was used for the examinations. The superplasticizers were added to the cement by dissolving them in the mixing water.

The OPC used in this study was a commercial OPC which is used very often in dry-mix mortar technology. A w/c-ratio of 0.5 and a 0.3 wt.% quantity – calculated on the basis of the dry cement – of the superplasticizer were used.

Heat flow experiments were performed using a commercial TAM Air calorimeter from TA Instruments. External stirring was performed using an electrical stirrer which allows a reproducible mixing. This means that the first hour of the signal has to be interpreted with care because of the possible disturbance of the signal when opening the calorimeter.

In situ X-ray experiments were performed using a D8 diffractometer equipped with a Lynx-Eye position sensitive detector. For each preparation 88 ranges were recorded during the first 22 h of hydration. Rietveld analysis [26] of the dry cement as well as of the cement pastes was performed using the software Topas V4.2 from Bruker (fundamental parameter approach [27]). All structures used, the quantities of the phases present in the dry cement, and the amounts normalized to a cement paste of a w/c ratio of 0.5 are shown in Table 1. Absolute quantities in the cement and cement pastes were calculated using the G-factor method [28,29]. This method involves using a well known crystalline standard (in our case silicon powder from a single crystal) to determine the calibration constant G for the diffractometer. This calibration constant is then used to calculate the concentration of each crystalline phase in the sample (here in the cement paste) taking into account the scale factor calculated by Rietveld refinement. A detailed evaluation of this method for the quantification of cement pastes is given elsewhere [30].

**Table 1**
Structures used for Rietveld refinement and mineralogical composition of the OPC with and without respect to the cement paste (w/c = 0.5).

| Phase | ICSD–code | wt.% dry cement | Expected amount in cement paste w/c = 0.5 [wt.%] |
|---|---|---|---|
| Silicon | 51688 [31] | Standard | Standard |
| Alite | 94742 [32] | 57.7 ± 1.2 | 38.5 ± 1.2 |
| Belite | 963 [33] | 11.7 ± 0.6 | 7.8 ± 0.6 |
| α`-$C_2S$ | [34] | 8.0 ± 0.5 | 5.3 ± 0.5 |
| $C_3A_{cub}$ | 1841 [35] | 5.6 ± 0.3 | 3.7 ± 0.3 |
| $C_3A_{ortho}$ | 100220 [36] | 4.8 ± 0.3 | 3.2 ± 0.3 |
| $C_4AF$ | 51265 [37] | 1.9 ± 0.2 | 1.3 ± 0.2 |
| Gypsum | 27221 [38] | 0.8 ± 0.1 | 0.5 ± 0.1 |
| Bassanite | 79529 [39] | 1.5 ± 0.1 | 1 ± 0.1 |
| Anhydrite | 16382 [40] | 3.0 ± 0.2 | 2 ± 0.2 |
| Calcite | 80869 [41] | 2.2 ± 0.2 | 1.5 ± 0.2 |
| Quartz | 174 [42] | 0.9 ± 0.1 | 0.6 ± 0.1 |
| Arcanite | 79777 [43] | 0.9 ± 0.1 | 0.6 ± 0.1 |
| Ettringite | 155395 [44] | – | – |
| Portlandite | 34241 [45] | – | – |
| Amorphous/misfitted | – | 1.0 ± 0.5 | 34 (water + misfitted) |

It was shown, using the thermodynamic software GEMS [46,47] and the thermodynamic data for cement phases [48], that the following equations should be used in order to calculate heat flow diagrams from XRD data [49].

$$C_3S + 3.9H \rightarrow C_{1.7}SH_{2.6} + 1.3CH \quad (1)$$

$$C_3A + 6H_2O \rightarrow 2Al(OH)_4^- + 2.5OH^- + 1.5Ca^{2+} + 1.5CaOH^+ \quad (2)$$

$$3CaSO_4 + 1.5OH^- \rightarrow 1.5Ca^{2+} + 1.5Ca(OH)^+ + 3{SO_4}^{2-} \quad (3)$$

$$3CaSO_4 * 2H_2O + 1.5OH^- \rightarrow 1.5Ca^{2+} + 1.5Ca(OH)^+ + 3SO_4^{2-} + 6H_2O \quad (4)$$

$$3Ca^{2+} + 3CaOH^+ + 2Al(OH)^{4-} + 3SO_4^{2-} + 2.5OH^- + 26H_2O \rightarrow \text{Ettringite} + 1.5OH^- \quad (5)$$

The enthalpies of reaction are shown in Table 2.

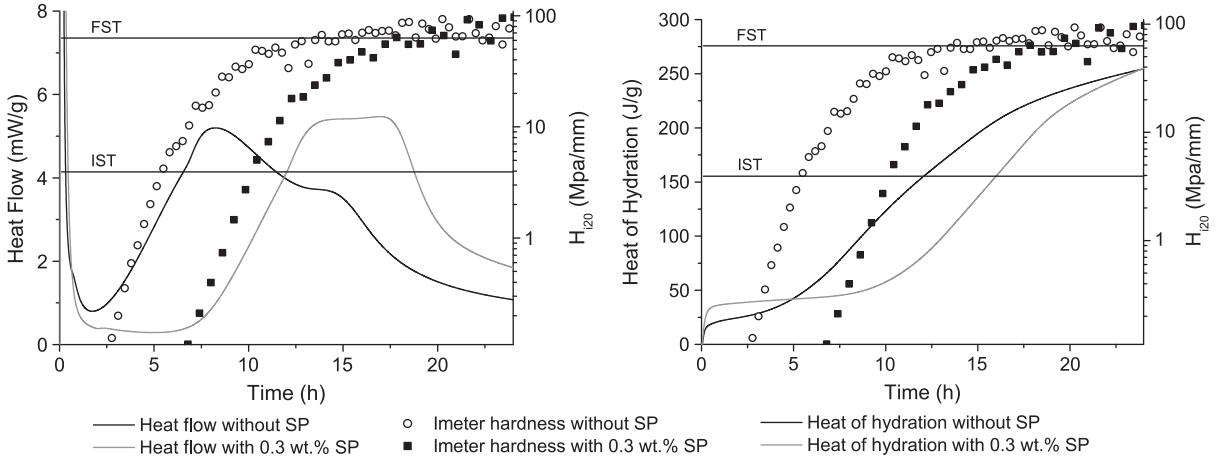


**Fig. 1.** Heat flow, heat of hydration and imeter hardness $H_{i20}$ of the cement used during hydration with and without [30] addition of superplasticizer.

**Table 2**
Enthalpies of reaction of dissolution and precipitation reactions.

| Reaction | Enthalpy |
|---|---|
| Eq. (1) (silicate reaction) | −561 J/$g_{Alite}$ |
| Eq. (2) (dissolution $C_3A$) | −868 J/$g_{C3A}$ |
| Eq. (3) (dissolution anhydrite) | −52 J/$g_{Anhydrite}$ |
| Eq. (4) (dissolution gypsum) | 57 J/$g_{Gypsum}$ |
| Eq. (5) (precipitation ettringite) | −214 J/$g_{Ettringite}$ |

The calculation of heat flow curves (HF) from XRD data generally follows Eq. (6)[50].

$$HF = \frac{\frac{\partial wt.\%\ phase}{\partial t}}{100} \times \Delta HR \quad (6)$$

where

$\frac{\partial wt.\%phase}{\partial t}$ derivation of the phase content curves

$\Delta H_R$ enthalpy of reaction

The setting time of the cements was determined using a Gillmore needle apparatus (imeter) (MSB Breitwieser, Augsburg, Germany). The cement paste was placed into a special sample holder and measured over the first 24 h of hydration (30 min intervals). In order to measure the hardness, the sample is automatically lifted against a needle of 212 g and a diameter of 0.692 mm. At each measurement point the time dependent weight reduction of the needle and the corresponding penetration depth is recorded and the hardness of the cement paste (the so-called "imeter-hardness") is calculated from the relation "strength per penetration depth", standardised by the diameter of the needle used. The resulting value $H_{i20}$ is calculated according to the following equation [51]:

$$H_{i20} = F_{max}/(d_{max} * A) \quad (7)$$

$H_{i20}$ imeter hardness according to method No.20 [Mpa/mm]
$F_{max}$ maximum value of the force acting during indentation
$d_{Fmax}$ penetration depth of the needle at maximum force
A cross-section area of the needle

For the used measurement system the initial setting time (IST) or final setting time (FST) according to ASTM C266 complies with an imeter value Hi20 (IST/FST) of 3.94 MPa/mm or 63.0 MPa/mm respectively. The setting times of the cement pastes were measured at 23 °C and >60% humidity. Each measurement was performed two times and the average value was calculated.

All experiments were performed at a temperature of 23 °C ± 0.5 °C.

## 3. Results

The plot of the heat of hydration, as well as the imeter hardness $H_{i20}$ in the same diagram, clearly show that there exists a close agreement between the heat evolution and the hardening of the cement paste. The plot of the heat flow and the increase of the imeter hardness over time also show that the hardening of the cement paste starts immediately after the beginning of the acceleration period. It can be clearly seen that the addition of the superplasticizer leads to a distinct retardation of the cement hydration. This means that the hardening process is correlatively significantly retarded.

It is known that the acceleration period resulting in the hardening of the cement paste is mainly defined by the silicate reaction. When

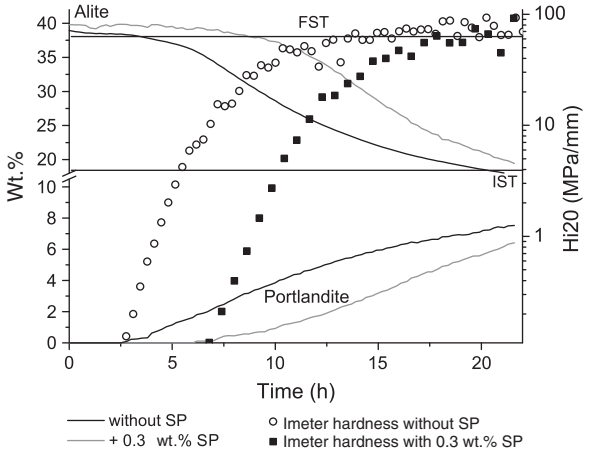


**Fig. 2.** Alite and portlandite content and imeter hardness during the hydration of the OPC with and without [30] addition of superplasticizer.

plotting the determined amounts of the phases alite and portlandite and the imeter hardness it can be seen that there is an obvious connection between the beginning of the dissolution of the phase alite/precipitation of portlandite and the start of the hardening of the cement paste Fig. 2). Since the superplasticizer clearly retards the dissolution of the phase alite, there can also be detected a distinct retardation of the hardening of the cement paste where the superplasticizer is added.

Not only the silicate reaction but also the aluminate reaction is significantly retarded where a superplasticizer is added to the cement (Fig. 3). The aluminate reaction, the reaction of the $C_3A$ with sulfate carriers and water forming ettringite, follows a defined pattern. Firstly, there is an immediate dissolution of $C_3A$ (here about 2 wt.%) which is traceable when considering the amount of $C_3A$ in the dry cement compared with the amount in the first XRD pattern of the cement paste (Table 1, Fig. 3, see also Fig. 6). There is no synchronous dissolution of two sulfate carriers detectable. Since no bassanite is detectable in the cement paste we assume that bassanite is dissolved firstly during the mixing of the cement. The anhydrite present in the cement seems to have three different dissolution rates. Firstly anydrite is dissolved before gypsum is dissolved until 2.5 h. Secondly anhydrite is dissolved after gypsum is completely dissolved between 6.6 h and 12.5 h. While the dissolution of gypsum can be detected there is no dissolution of anhydrite detectable. Thirdly, after 12.5 h there is a decrease in the reaction rate of the anhydrite dissolution detectable, although anhydrite is the last sulfate carrier available. We can find the same way of reaction of the aluminate reaction in the cement system with superplasticizer added, but significantly retarded.

The two most significant points in time described here (namely, the beginning of the second anhydrite dissolution, and the beginning of further $C_3A$ dissolution) occur significantly later in the system where superplasticizer is added (Fig. 3). The beginning of the anhydrite dissolution occurs at 12.5 h in comparison to 6.6 h in the system without addition of superplasticizers. The further dissolution of $C_3A$ is delayed for almost 4 h. Therefore, the sulfate depletion peak, which is caused by the dissolution of $C_3A$ and an accelerated ettringite precipitation [30,50] and which strongly depends on the amount of sulfate carriers available [52,53], occurs at later points in time where superplasticizer is added.

Indeed, it is worth mentioning that, after the retardation of the further $C_3A$ dissolution, the dissolution of the $C_3A$ takes place at a significantly faster rate when superplasticizer is present. This in turn gives rise to the circumstance that the first maximum, occurring during the main period at 7.5 h in the system without superplasticizer, and the second maximum, called the "sulfate depletion peak", tend to draw closer together in the system with superplasticizer added,

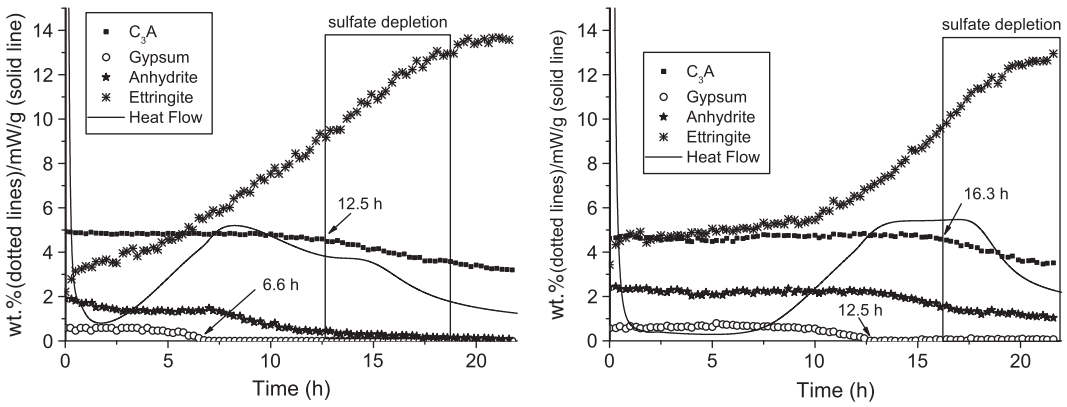


**Fig. 3.** Heat flow and phase content of the phases involved in the aluminate reaction during hydration of the OPC used with (right side) and without [30] (left side) superplasticizer.

so that it becomes difficult to distinguish the difference between both maxima.

The slowdown of the anhydrite dissolution, resulting in the further dissolution of the $C_3A$, also shows differences in both systems. In both systems – namely, with and without superplasticizer added – there is a significant slowdown of the visible anhydrite dissolution, although the amount of anhydrite remaining tends to differ. Nevertheless, it can be safely assumed that the slowdown of the dissolution of the last sulfate carrier available in combination with an ongoing ettringite precipitation results in a sulfate depletion in the pore solution and a resorption of sulfate ions from surfaces of the cement grains (see also [30]). This in turn allows the further dissolution of the $C_3A$. The further $C_3A$ dissolution occurs though there is still a significant amount of crystalline anhydrite present. We assume that there is an amount of anhydrite which is less reactive than the anhydrite which is dissolved quite fast before the further $C_3A$ reactions occurs. The worse reactivity of parts of the anhydrite might be caused by either bigger grains or better crystallinity of the anhydrite. The decelerated reaction rate of the anhydrite and the ongoing ettringite precipitation cause the sulfate depletion in the pore solution.

Fig. 4 shows the heat flow curves as measured as well as the calculated heat flow curves, using the results from in-situ X-ray analysis and the enthalpies of reaction as shown in Table 2. Neither the contribution of the gypsum dissolution nor that of the anhydrite dissolution was taken into account, since their contributions are below 0.1 mW. It can be seen that the heat flow as measured can be explained quite well, taking into account the findings from the X-ray experiments performed. It can be shown that the superplasticizer retards both the silicate reaction and the aluminate reaction. After a distinct retardation, both reactions emerge on a faster timeline. Hence, the calculated heat flow curve for cement with superplasticizer added does not show the two significant heat flow maxima during the main period between 2.5 and 20 h. However, the heat flow curve as actually measured can be resolved into two maxima.

Fig. 5, finally, shows the calculated heat flow curves from XRD data as well as the imeter hardness as measured. This figure demonstrates once more that the methods applied to the evaluation of the cement hydration confirm one another.

The retardation of the setting of the cement is caused by the suppression of both the silicate reaction and the aluminate reaction, which in turn leads to a retardation of the hardening of the cement paste.

## 4. Discussion

It can be shown that the superplasticizer retards both the silicate reaction and the aluminate reaction. The typical process of the aluminate reaction is not altered by addition of the superplasticizer, although all reactions are significantly retarded.

It is generally assumed that there obtains a preferred adsorption of anionic superplasticizers on those cement surfaces displaying opposite charge ($C_3A$, ettringite). This is obviously the requirement for the mode of action of superplasticizers.

On the basis of the research performed several mechanisms are thinkable.

The first mechanism which is conceivable is the complexation of $Ca^{2+}$-ions from pore solution. The withdrawal of the $Ca^{2+}$ ions from the pore solution by the superplasticizer might lead to a $Ca^{2+}$ depletion in the pore solution and result in the retardation of both, the silicate reaction and the aluminate reaction. $Ca^{2+}$ is an ion

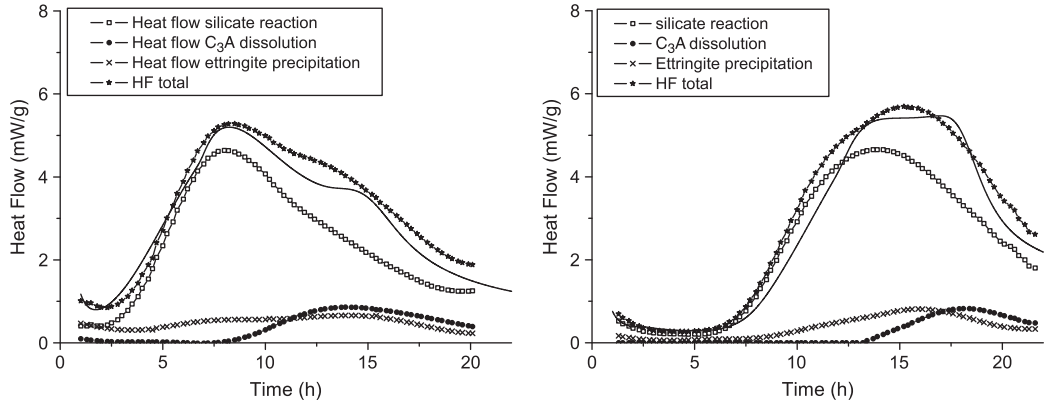


**Fig. 4.** Measured and calculated heat flow curves of the OPC used with (right) and without (left) superplasticizer added.

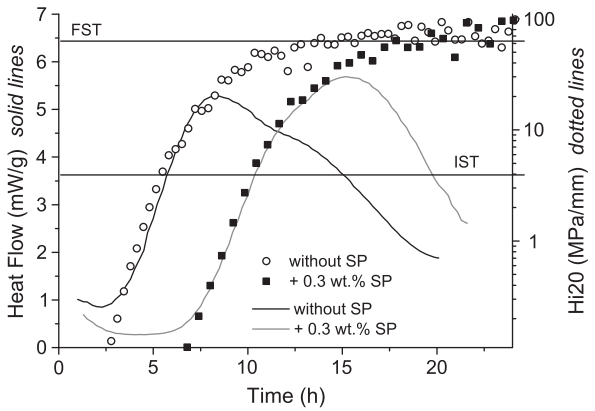


**Fig. 5.** Calculated heat flow curves and imeter hardness during the hydration of the OPC used with and without addition of superplasticizer.

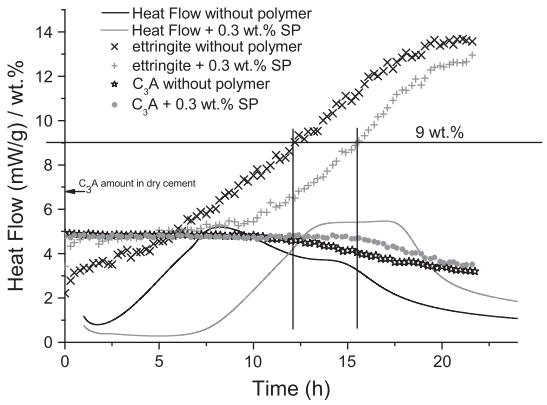


**Fig. 6.** Heat flow curves, ettringite content and $C_3A$ –content of the OPC with and without superplasticizer [30] added.

which is necessary for the precipitation of C–S–H, portlandite as well as ettringite. This hypothesis could, indeed, be confirmed by additional experimental data such as pore solution analysis.

But it is also conceivable that the superplasticizer added to the cement acts in another manner. It is furthermore thinkable that the superplasticizer added acts during the nucleation and growth phase of the hydration process. An adsorption of the superplasticizer on the nuclei of the hydrate phases and as a result the prevention of the growth of the hydrate phases might also be an explanation for the retardation of the hydration process.

Besides that, it is also thinkable that there is an adsorption of the macromolecules on the surfaces of the cement/clinker phases. The prevention of the dissolution of the anhydrous cement phases caused by the adsorption of the polymer is a possible result from this mechanism.

If the adsorption process is responsible for the retardation process of the cement further thoughts need to be given to the fact that both reactions, namely the silicate reaction and the aluminate reaction are retarded. According to other authors there is a preferred adsorption of the superplasticizers on the grain surfaces showing opposite charge [12,13]. Hence, the fact that both reactions are retarded in the same extent contradicts the findings that polymers show a preferred adsorption, unless the nuclei of all hydrate phases show same charge.

Our assumption is that the complexation of the $Ca^{2+}$-ions is the most conceivable mechanism responsible for the retardation of the cement hydration.

Concerning the sulfate depletion we want to make the following assumption. In contrast to the system without addition of superplasticizers, there is no precipitation of ettringite detectable in the system with superplasticizer added between 1 and 10 h. Since ettringite acts as a sulfate sink, a high $SO_4^{2-}$ concentration remains in the pore solution, especially at times after about 5 h. This prevents the further dissolution of the $C_3A$. Without consumption of sulfate from the pore solution there is no need for the further dissolution of any sulfate carrier.

For the cement used in the present investigation 9 wt.% quantity of ettringite is the critical quantity of ettringite in both systems required in order to reduce the $SO_4^{2-}$ concentration of the pore solution permanently, which in turn permits further $C_3A$ dissolution. This critical quantity of 9 wt.% is reached significantly later in the cement paste to which superplasticizer has been added (see Fig. 6). After the 9 wt.% of ettringite have been precipitated more sulfate is removed from pore solution by ettringite precipitation than sulfate is added by dissolution of any sulfate carrier. This in turn causes the depletion of sulfate in the pore solution and/or desorption of sulfate ions from grain surfaces and the further dissolution of $C_3A$.

Further thought needs to be given to the fact that, in the system to which superplasticizer is added, more ettringite tends to be precipitated immediately after mixing the cement with water, even though the precipitation of ettringite is clearly retarded in the subsequent stages of development.

Finally, the research performed shows that the retardation of cement hydration can be tracked by means of in-situ X-ray diffraction. All methods applied to the examination of the cementitious systems confirm each other. Hence, detailed statements concerning the retardation of cement hydration by a superplasticizer can be done.

## References

[1] R. Bayer, R. Lutz, Dry Mortars, Ullmann's Encyclopedia of Industrial Chemistry, 2009.
[2] A. Neville, P.-C. Aitcin, High performance concrete — an overview, Mater. Struct. 31 (1998) 111–117.
[3] P.-C. Aitcin, A. Neville, How the water–cement ration affects concrete strength, Cem. Int. (2003) 51–58.
[4] J.F. Young, A review of the mechanisms of set-retardation in Portland cement pastes containing organic admixtures, Cem. Concr. Res. 2 (1972) 415–433.
[5] S. Chandra, P. Flodin, Interactions of polymers and organic admixtures on Portland cement hydration, Cem. Concr. Res. 17 (1987) 875–890.
[6] H. Uchikawa, S. Hanehara, D. Sawaki, The role of steric repulsive force in the dispersion of cement particles in fresh paste prepared with organic mixture, Cem. Concr. Res. 27 (1997) 37–50.
[7] J. Plank, D. Vlad, A. Brandl, P. Chatziagorastou, Colloidal chemistry examination of the steric effect of polycarboxylate superplasticizers, Cem. Int. 3 (2005) 100–110.
[8] W. Prince, M. Espagne, P.-C. Aitcin, Ettringite formation; a crucial step in cement superplasticizer compatibility, Cem. Concr. Res. 33 (2003) 635–641.
[9] S. Erdogdu, Compatibility of superplasticizers with cements different in composition, Cem. Concr. Res. 30 (2000) 767–773.
[10] S.K. Agarwal, I. Masood, S.K. Malhotra, Compatibility of superplasticizers with different cements, Constr. Build. Mater. 14 (2000) 253–259.
[11] M.Y.A. Mollah, W.J. Adams, R. Schennach, D.L. Cocke, A review of cement-superplasticizer interactions and their models, Adv. Cem. Res. 12 (2000) 153–161.
[12] K. Yoshioka, E. Tazawa, K. Kawai, T. Enohata, Adsorption characteristics of superplasticizers on cement component minerals, Cem. Concr. Res. 32 (2002) 1507–1513.
[13] J. Plank, C. Hirsch, Impact of zeta potential of early cement hydration phases on superplasticizer adsorption, Cem. Concr. Res. 37 (2007) 537–542.
[14] J. Plank, D. Zhimin, H. Keller, F. Hössle, W. Seidl, Fundamental mechanisms for polycarboxylate intercalation into $C_3A$ hydrate phases and the role of sulfate present in cement, Cem. Concr. Res. 40 (2010) 45–57.
[15] S. Pourchet, C. Comparet, L. Nicoleau, A. Nonat, Influence of PC superplasticizer on tricalcium silicate hydration, 12th International Congress on the Chemistry of Cement - ICCC 2007., Montreal : Canada, 2007.
[16] B. Lothenbach, F. Winnefeld, R. Figi, The influence of superplasticizers on the hydration of Portland cement, 12th International Congress on the Chemistry of Cement - ICCC 2007., Montreal : Canada, 2007.
[17] J. Plank, M. Gretz, Study on the interaction between anionic and cationic latex particles and Portland cement, Colloids Surf., A: Physicochem. Eng. Aspects 330 (2008) 227–233.
[18] J. Plank, P. Chatziagorastou, C. Hirsch, New model describing distribution of adsorbed superplasticizer on the surface of hydrating cement grain, J. Build. Mater. 10 (2007) 7–13.
[19] J.A. Larbi, J. Bijen, Interaction of polymers with Portland cement during hydration — a study of the chemistry of the pore solution of polymer-modified cement systems, Cem. Concr. Res. 20 (1990) 139–147.

[20] P.J. Andersen, D.M. Roy, J.M. Gaidis, W.R. Grace, The effects of adsorption of superplasticizers on the surface of cement, Cem. Concr. Res. 17 (1987) 805–813.
[21] G. Chiocchio, A.E. Paolini, Optimum time for adding superplasticizer to Portland cement pastes, Cem. Concr. Res. 15 (1985) 901–908.
[22] M. Daimon, D.M. Roy, Rheological properties of cement mixes: I. Methods, preliminary experiments, and adsorption studies, Cem. Concr. Res. 8 (1978) 753–764.
[23] M. Daimon, D.M. Roy, Rheological properties of cement mixes: II. Zeta potential and preliminary viscosity studies, Cem. Concr. Res. 9 (1979) 103–109.
[24] F. Winnefeld, A. Zingg, L. Holzer, R. Figi, J. Pakusch, S. Becker, Interaction of polycarboxylate-based superplasticizers and cements: influence of polymer structure and $C_3A$-content of cement, Cem. Concr. Compos. 29 (2007) 251–262.
[25] K. Yamada, T. Takahashi, S. Hanehara, M. Matsuhisa, Effects of the chemical structure on the properties of polycarboxylate-type superplasticizers, Cem. Concr. Res. 30 (2000) 197–207.
[26] H.M. Rietveld, A profile refinement method for nuclear and magnetic structures, J. Appl. Crystallogr. 2 (1969) 65–71.
[27] A.A. Kern, A.A. Coelho, A new fundamental parameters approach in profile analysis of powder data, Powder Diffr. (1998) 144–151.
[28] B.H. O´Connor, M.D. Raven, Application of the rietveld refinement procedure in assaying powdered mixtures, Powder Diffr. 3 (1988) 2–6.
[29] D. Jansen, Ch. Stabler, F. Goetz-Neunhoeffer, S. Dittrich, J. Neubauer, Does ordinary Portland cement contain amorphous phase? A quantitative study using an external standard method, Powder Diffr. 26 (2011) 31–38.
[30] D. Jansen, F. Goetz-Neunhoeffer, Ch. Stabler, J. Neubauer, A remastered external standard method applied to the quantification of early OPC hydration, Cem. Concr. Res. 41 (2011) 602–608.
[31] D.M. Többens, N. Stuesser, K. Knorr, H.M. Mayer, G. Lampert, The new high-resolution neutron powder diffractometer at the Berlin neutron scattering center, Mater. Sci. Forum 378–381 (2001) 288–293.
[32] A.G. De La Torre, S. Bruque, J. Campo, M.A.G. Aranda, The superstructure of $C_3S$ from synchrotron and neutron powder diffraction and its role in quantitative phase analysis, Cem. Concr. Res. 32 (2002) 1347–1356.
[33] K.H. Jost, B. Ziemer, R. Seydel, Redetermination of the structure of β-dicalcium silicate, Acta Crystallogr., Sect. B: Struct. Crystallogr. Cryst. Chem. 33 (1977) 1696–1700.
[34] R. Mueller, Stabilisierung verschiedener Dicalciumsilikat-Modifikationen durch den Einbau von Phosphat: Synthese, Rietveld-analyse, Kalorimetrie, Diplom-thesis (2001) University of Erlangen.
[35] P. Mondal, J. Jeffery, The crystal structure of tricalcium aluminate, $Ca_3Al_2O_6$, Acta Crystallogr., Sect. B: Struct. Crystallogr. Cryst. Chem. 31 (1975) 689–697.
[36] Y. Takéuchi, F. Nishi, Crystal–chemical characterization of the $Al_2O_3$–$Na_2O$ solid-solution series, Z. Kristallogr. 152 (1980) 259–307.
[37] A.C. Jupe, J.K. Cockcroft, P. Barnes, S.L. Colston, G. Sankar, C. Hall, The site occupancy of Mg in the brownmillerite structure and its effect on hydration properties: an X-ray/neutron diffraction and EXAFS study, J. Appl. Crystallogr. 34 (2001) 55–61.
[38] B.F. Pedersen, Neutron diffraction refinement of the structure of gypsum, Acta Crystallogr. Sect. B, Struct. Crystallogr. Cryst. Chem. 38 (1982) 1074–1077.
[39] H. Weiss, M.F. Bräu, How much water does calcined gypsum contain? Angew. Chem. Int. Ed. 48 (2009) 3520–3524.
[40] A. Kirfel, G. Will, Charge density in anhydrite $CaSO_4$, from X-ray and neutron diffraction measurements, Acta Crystallogr., Sect.B: Struct. Crystallogr. Cryst. Chem. 36 (1980) 288–2890.
[41] E.N. Maslen, V.A. Streltsov, N.R. Streltsova, Electron density and optical anisotropy in rhombohedral carbonates. III. Synchroton X-ray studies of $CaCO_3$, $MgCO_3$ and $MnCO_3$, Acta Crystallogr., Sect. B: Struct. Sci. 51 (1995) 929–939.
[42] Y. Le Page, G. Donnay, Refinement of the crystal structure of low-quartz, Acta Crystallogr., Sect.B: Struct. Crystallogr. Cryst. Chem. 32 (1976) 2456–2459.
[43] K. Ojima, Y. Hishihata, A. Sawada, Structure of potassium sulfate at temperatures from 296 K down to 15 K, Acta Crystallogr., Sect. B: Struct. Sci. 51 (1995) 287–293.
[44] F. Goetz-Neunhoeffer, J. Neubauer, Refined ettringite structure for quantitative X-ray diffraction analysis, Powder Diffr. 21 (2006) 4–11.
[45] W.R. Busing, H.A. Levy, Neutron diffraction study of calcium hydroxide, Acta Crystallogr., Sect. B: Struct. Sci. 42 (1986) 51–55.
[46] Kulik, D., GEMS-PSI 3.0 2010, available at http://gems.web.psi.ch/. PSI-Villigen, Switzerland.
[47] W. Hummel, U. Berner, E. Curti, F.J. Pearson, T. Thoenen, Nagra/PSI Chemical Thermodynamic Data Base 01/01. 2002, USA, also published as Nagra Technical Report NTB 02-16, Wettingen, Switzerland, Universal Publishers/uPUBLISH.com, 2002, p. 565.
[48] B. Lothenbach, T. Matschei, G. Möschner, F.P. Glasser, Thermodynamic modeling of the effect of temperature on the hydration and porosity of Portland cement, Cem. Concr. Res. 38 (2008) 1–18.
[49] D. Jansen, F. Goetz-Neunhoeffer, B. Lothenbach, J. Neubauer, The early hydration of Ordinary Portland Cement (OPC): An approach comparing measured heat flow with calculated heat flow from QXRD, Cem. Concr. Res. (2011) doi:10.1016/j.cemconres.2011.09.001.
[50] C. Hesse, F. Goetz-Neunhoeffer, J. Neubauer, A new approach in quantitative in-situ XRD of cement pastes: Correlation of heat flow curves with early hydration reactions, Cem. Concr. Res. 41 (2010) 123–128.
[51] G. Berger, Ch. Ullner, G. Neumann, H. Marx, New characterization of setting times of alkali containing calcium phosphate cements by using an automatically working device according to Gillmore needle test, Key Eng. Mater. 309–311 (2006) 825–828.
[52] P. Sandberg, L.R. Roberts, Studies of cement-admixture interactions related to aluminate hydration control by isothermal calorimetry, Am. Conr. Inst. 217 (2003) 529–542.
[53] W. Lerch, The influence of gypsum on the hydration and properties of Portland cement pastes, Am. Soc. Test. Mater. 46 (1946) 1252–1297.